JOURNAL OF HIGH-FREQUENCY COMMUNICATION TECHNOLOGIES
Vol. 01 (02) (2023), pp.55-63
https://doi.org/10.58399/INHK8527

Optically Transparent MIMO Antenna with Polarization Diversity

Devisowjanya Potti[1], **Kirubaveni Savarimuthu**[2*], **Hema Y**[3], **Ishwarya Devi R**[4]

[1] Department of ECE, Amrita School of Engineering, Chennai, 601103, India
[2,3,4] Department of ECE, Sri Sivasubramaniya Nadar College of Engineering, Chennai-603110, India *E-mail address: devi.sowjanya469@gmail.com, kirubavenis@ssn.edu.in, rpnyallanki1967@gmail.com, iswaryarajkumar7@gmail.com*

Abstract

An optically transparent UWB antenna with polarization diversity for the use of automotive communications is presented in this paper. The novel two element antenna operates at the frequency range of 2.5-8 GHz with dimension $45 \times 45\ mm^2$ and peak gain 1.2 dBi. Antenna elements are placed orthogonally to achieve polarisation diversity. The proposed antenna is placed on a soda lime glass substrate that has a permittivity of 7.3 and thickness of 2.2 mm. The radiator of the antenna is made of FTO with sheet resistance 6 Ω/sq. The diversity gain of the proposed antenna is greater than 9.9 and ECC value is lesser than 0.02 for the frequency range of 3-8 GHz. The isolation between the antenna elements is more than 15 dB without any complex decoupling structures between them.

Keywords: *Aluminium-doped Zinc oxide (AZO); Multiple-input-multiple-output (MIMO); Transparent antennas; UWB antenna; Polarisation diversity*

1. Introduction

Recently, wireless communication has become a wide range of interest for research. Automobiles are aimed at providing an extensive communication service. They are expected to be installed with a good range of wireless communication systems and multimedia products. Automotive antennas are equipped in automobiles with the uninterrupted transmission of radio waves for ceaseless communication. Automobiles are expected to have antennas operating at different frequency ranges to fulfil the above-mentioned requirements. Ultra-wide band (UWB) would be a better option. It covers a wide range of frequencies from 3.1 to 10.6 GHz, which was allocated by the FCC. UWB technology provides a high data rate and also consumes a very low amount of power. High-speed mobile communications, in-car sensor network communication, automotive localization and tracking with high spatial resolution, emergency services and roadside assistance are some promising applications of UWB. Like any other wireless communication systems, UWB also suffers from the problem of multipath propagation. The fast movement of the vehicle causes impairments in the data rate and link quality. These impairments are caused by multipath propagation and fading. To overcome these problems, MIMO/Polarisation diversity is introduced. They improve the channel capacity and link quality. They also alleviate the effects of multipath fading.

Several UWB MIMO antennas with two antenna elements are proposed in (Dong et al., 2017), (Ren et al., 2014), (Mao and Chu, 2014), (Luo et al., 2015), (Zhang et al., 2009), (Liu et al.,

*Corresponding author
Received: 17^{th}, December 2022, Revised: 12^{th} March, 2023 Accepted: 22^{nd} March 2023 and available online 10^{th} April 2023

This work is licensed under a Creative Commons Attribution 4.0 License(CC BY 4.0).
For more information, see https://creativecommons.org/licenses/by/4.0/

BLUE MARTIN PRESS

2015), (Iqbal et al., 2017), (Lin et al., 2017) and (Liu et al., 2014). According to the author limited research has been conducted on the UWB MIMO antenna with two antenna elements. The coupling between the antennas in the MIMO system alleviates the performance. It can be reduced by increasing the isolation. High isolation is achieved by etching slots or adding stubs. A defective ground structure with an I-shaped slot and a pair of L-shaped stubs were employed to improve isolation (Dong et al., 2017). In (Ren et al., 2014) a narrow rectangular slot is etched to reduce the mutual coupling. A T-shaped slot and an extended stub improved isolation in (Mao and Chu, 2014). A T-shaped slot and a line slot (Luo et al., 2015) provided high isolation between the radiators. A tree-like structure is employed on the ground for achieving wideband isolation (Zhang et al., 2009). In (Liu et al., 2015), a T-shaped ground stub and in (Iqbal et al., 2017), F-shaped stubs were added to reduce mutual coupling. To improve isolation, a carbon film is used (Lin et al., 2017) and (Liu et al., 2014) achieves high isolation without decoupling structures; however, the Envelope Correlation Coefficient (ECC) is higher than others. The ECC should be ideally zero for uncorrelated diversity antenna. Practically, it should be less than 0.25 (Liu et al., 2014) and (Alsath and Kanagasabai, 2015) study has ECC below 0.004, which is lesser than the other studies (Ren et al., 2014), (Liu et al., 2015), (Iqbal et al., 2017), (Lin et al., 2017) and (Liu et al., 2014) but it uses decoupling structures for improved isolation. Few optically transparent MIMO antennas are proposed in (Potti et al., 2021), (Li et al., 2017) and (So et al., 2020). These antennas explored the spatial diversity of MIMO antennas. The antenna proposed in (Desai et al., 2019) studied the polarization diversity of the MIMO antenna at WiMax and WLAN bands. The antenna proposed in this paper studied the polarization diversity of the antenna in a wideband range. The UWB MIMO should have high isolation to avoid coupling between the radiators, low ECC for better diversity performance, wide bandwidth, and small size. To the best of the author's knowledge, research has yet to be reported on optically transparent UWB two-element antenna with polarisation diversity in wideband range to date. This paper proposes a novel optically transparent

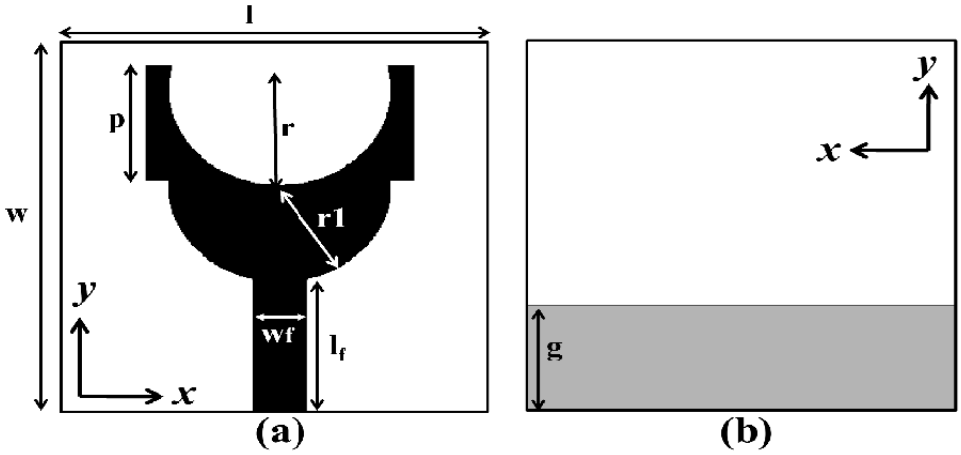

Figure 1. Proposed single element UWB antenna: (a) front view (b) rear view
Optimized dimensions: l=22.5 mm w=22.5 mm, p=7 mm, r=5.8 mm, r1=5.8 mm l_f =8mm, wf=2.8 mm, g=6.5 mm

UWB-polarisation diversity antenna with two antenna elements for automotive communications is proposed. Placing multiple antennas improves communication service, but causes space constraints and affects the vehicles'. Conventional antennas are opaque in nature. They are fabricated with metal on dielectric substrates. The transparency is obtained using transparent conducting oxides (TCOs). Radiating patch and ground plane of the antenna are made up of TCOs. Although using the TCOs, the antennas achieve high transparency, but have poor conductivity, affecting gain and efficiency. The addition of metal dopants will overcome the conductivity issues. It increases the conductivity and also maintains transparency. They can be integrated into any part of the vehicle without affecting their look. The transparent UWB MIMO antenna presented in this paper is fabricated on soda lime glass. The radiator is made up of AZO film (aluminium-doped zinc oxide). Also, the ground is made up of AZO in addition to FTO (fluorine-doped tin oxide).

The rest of the paper is organized as follows: Section 2 details the design of the transparent two element UWB MIMO antenna. Section 3 discusses the results of the proposed antenna.

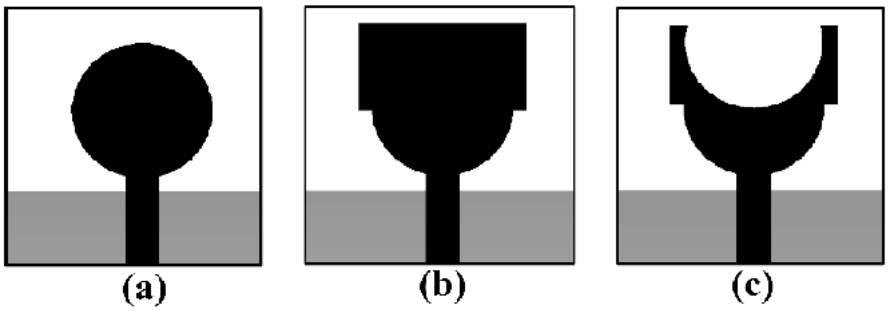

Figure 2. Evolution of a single element UWB antenna: (a) evolution 1, (b) evolution 2, and (c) proposed antenna

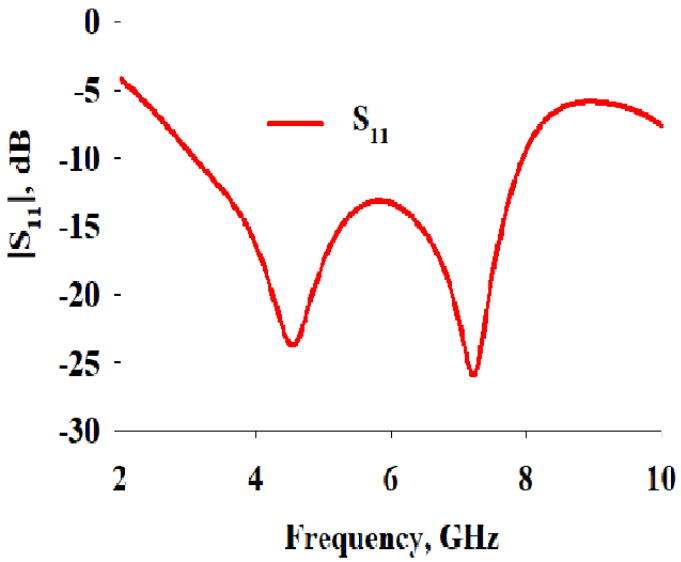

Figure 3. Reflection coefficients characteristics of a single element UWB antenna

2. Single Element Antenna

The proposed single element is a monopole antenna that operates from 3 to 8 GHz. The geometry of the monopole along with its reflection coefficient characteristics are presented in the below section. A simple monopole antenna is shown in Fig. 1. The antenna is designed on a soda lime glass substrate with a permittivity of 7.3, and a thickness of 2.2 mm, respectively. The radiator of the antenna is made of AZO film to attain transparency. The AZO film has a sheet resistance of 6 Ω/sq. and a thickness of 600 nm. To increase the conductivity, the bottom side of the substrate is coated with both FTO and AZO, reducing the sheet resistance to 4 Ω/sq. The designed UWB antenna consists of a circular monopole with a rectangular stub on the top as shown in Fig. 2(a). A rectangular stub was added on the top of the radiator to increase the bandwidth at higher frequencies as shown in Fig.2(b). The width of the rectangular slot was gradually varied between 12 mm and 14 mm. An increase in the width resulted in an increased gain. Therefore, the width of the rectangular slot was fixed at 14 mm. A semi-circular slot is etched out of the radiator's rectangular portion as shown in Fig.3(c), providing increased bandwidth and a further increase in the gain. The evolution of the antenna is shown in Fig.2. The radiator is fed by a

microstrip feed line of length 8 mm and width 2.8 mm. The overall dimension of the antenna is $22.5 \times 22.5\ mm^2$. The proposed antenna operates over a bandwidth of 5 GHz as shown in Fig.3.

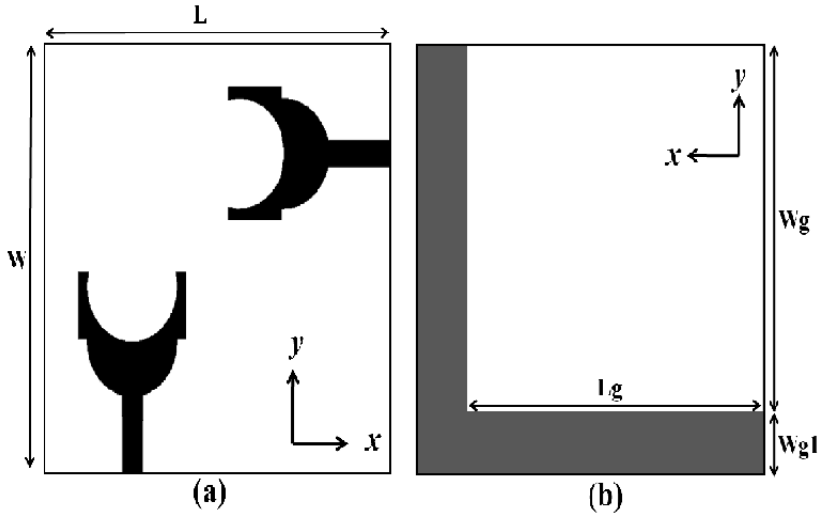

Figure 4. Proposed UWB MIMO antenna: (a) front view, (b) rear view
Optimized dimensions: L=45 mm, W=45 mm, Lg=38.5 mm, Wg=38.5 mm, Wg1=6.5 mm

3. UWB MIMO Antenna

The geometry of the proposed two-element UWB MIMO antenna with an overall dimension of $45 \times 45\ mm^2$ is shown in Fig.4. To enhance the channel capacity and to decrease the effects of multipath fading, the two radiating elements are placed orthogonal to each other. A square-shaped slot is etched out on the other side of the substrate to form an L-shaped partial ground to improve bandwidth and impedance matching at low frequencies. The proposed UWB antenna operates from 3 to 8 GHz as shown in Fig.5 and the isolation between the antennas is greater than 18 dB over the entire operating frequency range. The surface current distribution of the MIMO antenna in Fig.6 shows that the isolation between the antenna is high without adding any isolation structures.

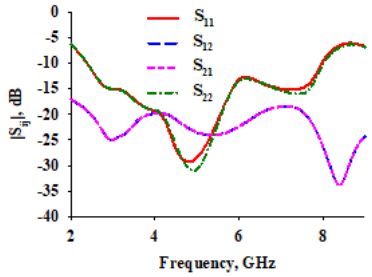

Figure 5. Simulated reflection and isolation coefficients characteristics of UWB MIMO antenna

4. Results and Discussion

The UWB MIMO antenna is fabricated using the sputtering technique. The top and bottom layers of the transparent conductive oxides are sputtered on the soda lime glass substrate using dc magnetron sputtering. The SMA connector is connected using the cold soldering method. The fabricated prototype is shown in Fig.7. The fabricated antenna is tested for impedance characteristics using VNA and radiation characteristics are tested in an anechoic chamber.

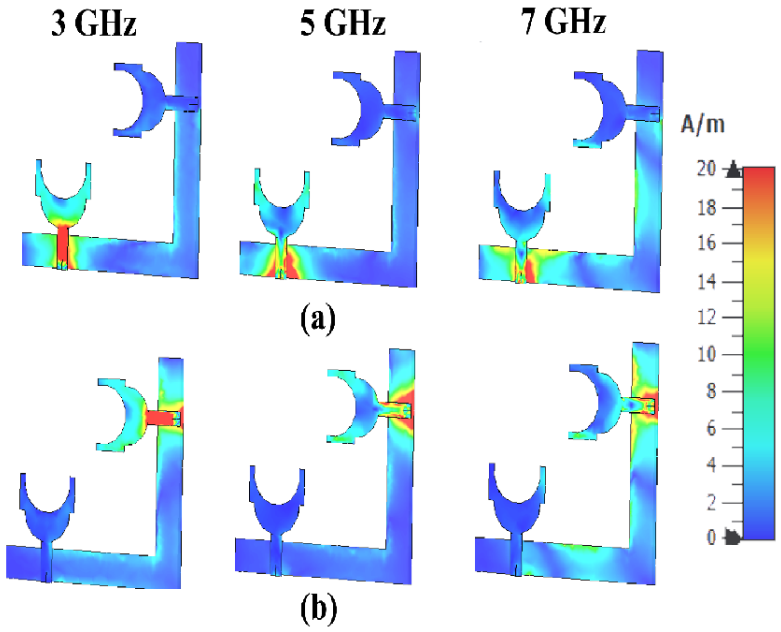

Figure 6. Surface current distribution of the UWB MIMO antenna at 3, 5, and 7 GHz with (a) port 1 excited and (b) port 2 excited

4.1. Impedence Characteristics

The fabricated UWB MIMO antenna exhibits a bandwidth of 5.5 GHz extending from 2.5 GHz to 8 GHz. The simulated reflection coefficient characteristics and isolation characteristics of the proposed antenna are shown in Fig.8. A good isolation of more than 25 dB is observed between the radiators without any decoupling structures between them for the entire frequency range.

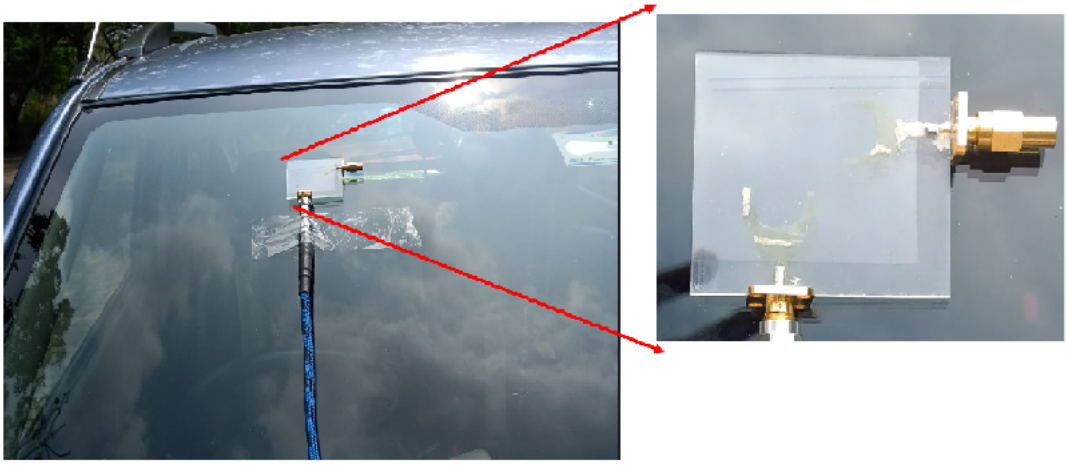

Figure 7. Fabricated prototype of the MIMO antenna

4.2. Radiation Characteristics

The simulated and measured radiation pattern characteristics of the proposed antenna at 5, 6, and 7 GHz with port 1 excited and port 2 terminated with 50 Ω impedance are shown in Fig.9. The simulated and measured realized gain and radiation efficiency of the proposed antenna are shown in Fig.10. The measured peak realized gain of the antenna is 1.19 dBi. The radiation efficiency of the proposed antenna varies between 39% and 49% with peak efficiency at 5 GHz.

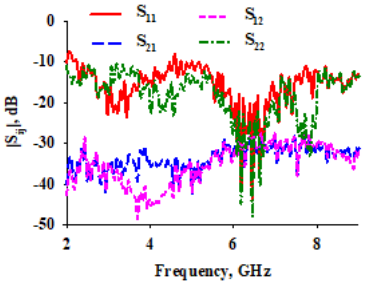

Figure 8. Measured reflection and isolation coefficients characteristics of UWB MIMO antenna

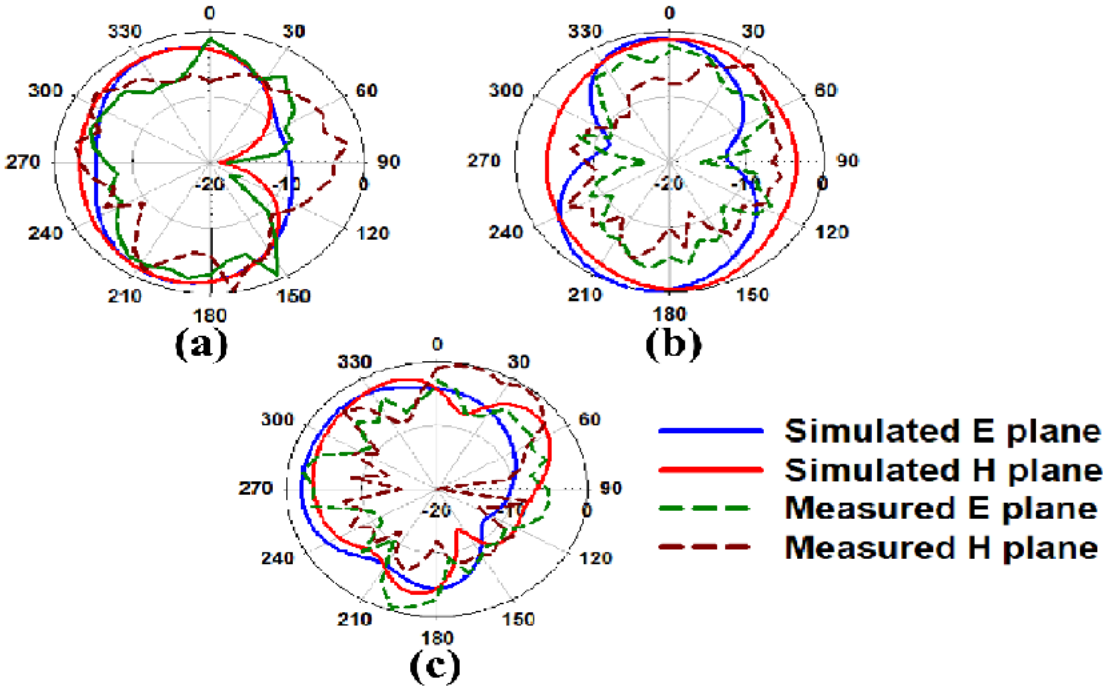

Figure 9. Simulated and measured normalized radiation pattern at port 1 (a) 3 GHz, (b) 5 GHz, and (c) 7 GHz

4.3. MIMO Performance Parameters

The parameters that determine the performance of the MIMO antenna are Envelope Correlation Coefficient (ECC), Diversity Gain (DG), Mean Effective Gain (MEG), and Channel Capacity Loss (CLL). The correlation between the antennas is measured by the parameter ECC (ρ_{ij}). The standard value of ECC should be less than 0.5. The ECC and diversity gain value for the proposed two-element antenna can be calculated using a far-field radiation pattern as shown in equations 1 and 2, respectively,

$$ECC = |\rho_{ij}|^2 = \frac{|\iint [E_i(\theta,\varphi) * E_j(\theta,\varphi) d\Omega]^2}{\iint |E_i(\theta,\varphi)|^2 d\Omega \iint |E_j(\theta,\varphi)|^2 d\Omega} \tag{1}$$

$$Diversity\ Gain(DG) = 10\sqrt{1 - |\rho_{ij}|^2} \tag{2}$$

where E_i and E_j are the radiated fields of the i^{th} and j^{th} antenna. The simulated ECC of the proposed antenna is less than 0.02 over the entire operating frequency range as shown in Fig.11. The simulated diversity gain of the proposed antenna is greater than 9.9 over the operating frequency range as shown in Fig.11 which shows that it has less loss in transmission power.

The mean received power is analyzed using mean effective gain (MEG) which is given by

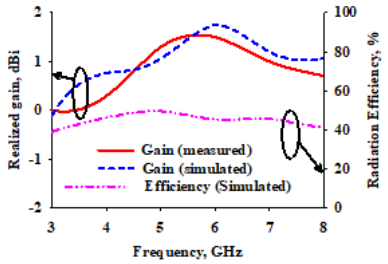

Figure 10. Simulated and measured realized gain and simulated efficiency of the proposed MIMO antenna

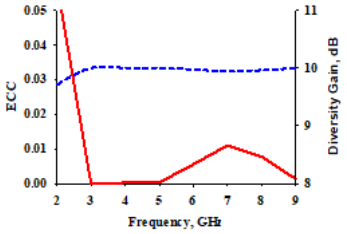

Figure 11. Simulated ECC and diversity gain of the proposed antenna

equation 3.

$$MEG_i = 0.5(1 - \sum_{j=1}^{K} |S_{ij}|) \tag{3}$$

where S_{ii} and S_{ij} are the reflection and isolation coefficients of the antenna. The simulated and calculated mean effective gain of the antenna are shown in Fig.12. To obtain a good diversity performance, the MEG should be $-3 \leq MEG(dB) \leq -12$. If the antennas are 100% efficient, then maximum MEG (dB) is -3 dB (Fakharian et al., 2022). The proposed antenna MEG is between $-3 \leq MEG(dB) \leq -5$ as shown in Fig.12 which shows the proposed antennas has suitable MEG.

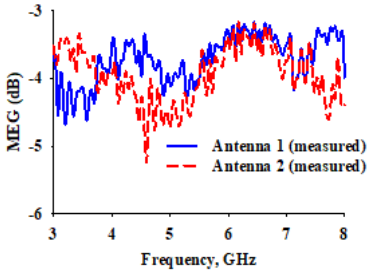

Figure 12. Measured MEG (dB) of the proposed antenna

4.4. Comparison of the MIMO antenna with other MIMO antennas in the literature

From Table 1, it is observed that

1. The antenna is compact in size as compared to (Dong et al., 2017), (Mao and Chu, 2014), (Zhang et al., 2009), (Iqbal et al., 2017) and (Lin et al., 2017).

2. The ECC of the proposed antenna is lesser than (Ren et al., 2014), (Liu et al., 2015), (Iqbal et al., 2017) and (Liu et al., 2014).

3. The diversity gain of the proposed antenna is greater than (Lin et al., 2017).

4. The proposed antenna is transparent in nature when compared with others.

Table 1. Comparison of Proposed Design with Literature

References	Size (mm)	Frequencies (GHz)	Gain	ECC	DG	Transparent
(Dong et al., 2017)	$0.32\lambda \times 0.56\lambda$	3.28-12	-	-	-	No
(Ren et al., 2014)	$0.3\lambda \times 0.3\lambda$	2.9-12	1.7-4.2	< 0.4	-	No
(Mao and Chu, 2014)	$0.42\lambda \times 0.42\lambda$	3.2-10	-	-	-	No
(Luo et al., 2015)	$0.22\lambda \times 0.26\lambda$	3.1-10.6	3.8	< 0.04	-	No
(Zhang et al., 2009)	$0.36\lambda \times 0.41\lambda$	3.1-10.6	3.1	< 0.01	-	No
(Liu et al., 2015)	$0.19\lambda \times 0.31\lambda$	2.6-11	1-5	< 0.06	-	No
(Iqbal et al., 2017)	$0.41\lambda \times 0.25\lambda$	2.5-14.5	0.3-4.3	< 0.04	-	No
(Lin et al., 2017)	$0.41\lambda \times 0.33\lambda$	2.5-11	> 2.11	< 0.01	> 7.4	No
(Liu et al., 2014)	$0.21\lambda \times 0.29\lambda$	2.14-11.4	6.5	< 0.25	-	No
This Paper	$0.37\lambda \times 0.37\lambda$	2.5-8	0 - 2	< 0.02	> 9.9	Yes

5. Conclusion

A novel transparent MIMO antenna is proposed for UWB automotive applications. The antenna operates at a frequency of 3 to 8 GHz, making it suitable for UWB applications. The isolation between the antennas is more than 17 dB without adding any decoupling structures. It has an ECC value of less than 0.02 and a diversity gain greater than 9.9 dB, making it a good candidate for the UWB MIMO antenna. The simulated and measured results are well in accordance with each other. It has an omnidirectional radiation pattern with a measured peak realized gain of 1.9 dBi and simulated peak radiation efficiency of 49% at 5 GHz. The transmittance of the antenna is greater than 72% so that it can be installed on the car's windshields.

References

Alsath, M. G. N and Kanagasabai, M. Compact uwb monopole antenna for automotive communications. *IEEE Transactions on Antennas and Propagation*, 63, 2015. ISSN 0018926X. doi: 10.1109/TAP.2015.2447006.

Desai, A; Upadhyaya, T; Palandoken, M, and Gocen, C. Dual band transparent antenna for wireless mimo system applications. *Microwave and Optical Technology Letters*, 61, 2019. ISSN 10982760. doi: 10.1002/mop.31825.

Dong, Y; Li, Y; Yu, K, and Wang, Y. High isolation design of a two-element planar uwb-mimo monopole antenna. 2017. doi: 10.23919/ROPACES.2017.7916030.

Fakharian, M. M; Alibakhshikenari, M; See, C. H, and Abd-Alhameed, R. A high gain multiband offset mimo antenna based on a planar log-periodic array for ku/k-band applications. *Scientific Reports*, 12, 2022. ISSN 20452322. doi: 10.1038/s41598-022-07866-1.

Iqbal, A; Saraereh, O. A; Ahmad, A. W, and Bashir, S. Mutual coupling reduction using f-shaped stubs in uwb-mimo antenna. *IEEE Access*, 6, 2017. ISSN 21693536. doi: 10.1109/ACCESS.2017.2785232.

Li, Q. L; Cheung, S. W; Wu, D, and Yuk, T. I. Optically transparent dual-band mimo antenna using micro-metal mesh conductive film for wlan system. *IEEE Antennas and Wireless Propagation Letters*, 16, 2017. ISSN 15361225. doi: 10.1109/LAWP.2016.2614577.

Lin, G. S; Sung, C. H; Chen, J. L; Chen, L. S, and Houng, M. P. Isolation improvement in uwb mimo antenna system using carbon black film. *IEEE Antennas and Wireless Propagation Letters*, 16, 2017. ISSN 15361225. doi: 10.1109/LAWP.2016.2570301.

Liu, L; Cheung, S. W, and Yuk, T. I. Compact mimo antenna for portable uwb applications with band-notched characteristic. *IEEE Transactions on Antennas and Propagation*, 63, 2015. ISSN 0018926X. doi: 10.1109/TAP.2015.2406892.

Liu, X. L; Wang, Z. D; Yin, Y. Z; Ren, J, and Wu, J. J. A compact ultrawideband mimo antenna using qsca for high isolation. *IEEE Antennas and Wireless Propagation Letters*, 13, 2014. ISSN 15361225. doi: 10.1109/LAWP.2014.2340395.

Luo, C. M; Hong, J. S, and Zhong, L. L. Isolation enhancement of a very compact uwb-mimo slot antenna with two defected ground structures. *IEEE Antennas and Wireless Propagation Letters*, 14, 2015. ISSN 15361225. doi: 10.1109/LAWP.2015.2423318.

Mao, C. X and Chu, Q. X. Compact coradiator uwb-mimo antenna with dual polarization. *IEEE Transactions on Antennas and Propagation*, 62, 2014. ISSN 0018926X. doi: 10.1109/TAP.2014.2333066.

Potti, D; Tusharika, Y; Alsath, M. G. N; Kirubaveni, S; Kanagasabai, M; Sankararajan, R; Narendhiran, S, and Bhargav, P. B. A novel optically transparent uwb antenna for automotive mimo communications. *IEEE Transactions on Antennas and Propagation*, 69(7):3821–3828, 2021. doi: 10.1109/TAP.2020.3044383.

Ren, J; Hu, W; Yin, Y, and Fan, R. Compact printed mimo antenna for uwb applications. *IEEE Antennas and Wireless Propagation Letters*, 13, 2014. ISSN 15361225. doi: 10.1109/LAWP.2014.2343454.

So, K. K; Chen, B. J, and Chan, C. H. Microwave and millimeter-wave mimo antenna using conductive ito film. *IEEE Access*, 8, 2020. ISSN 21693536. doi: 10.1109/ACCESS.2020.3037900.

Zhang, S; Ying, Z; Xiong, J, and He, S. Ultrawideband mimo/diversity antennas with a tree-like structure to enhance wideband isolation. *IEEE Antennas and Wireless Propagation Letters*, 8, 2009. ISSN 15361225. doi: 10.1109/LAWP.2009.2037027.